Effect of stress on the growth of concentric grains and pores embedded in a binary alloy matrix

Jérôme Colin*
Department of Mathematics, University of California–Irvine, Irvine, California 92697-3875, USA
(Received 11 July 2008; published 14 January 2009)

The isothermal growth of a spherical grain from its melt filling a spherical pore embedded in a binary alloy matrix under stress has been investigated as well as the dissolution of the matrix, assuming solute diffusion only proceeds in the liquid phase. Neglecting the effects of pressure in the liquid, gravity, interfacial stress, and density changes, the applied stress has been identified as the driving force for the grain to grow and the matrix to dissolve through isothermal solidification and melting processes, respectively. A linear stability analysis has been then performed and the stress has been found to be responsible for the destabilization of both fronts leading in particular to the development of a delayed roughness on the stress-free grain interface.

DOI: 10.1103/PhysRevB.79.012103 PACS number(s): 81.10.Aj, 62.20.D−, 81.10.Fq, 66.10.C−

The melting and freezing phenomena in pores and nanopores embedded in a solid matrix have been intensively studied from both experimental and theoretical points of view because of their role in a number of engineering fields and processes, including record information technology[1] and performance degradation of polymer electrolyte membrane hydrogen fuel cells.[2] More precisely, the effects of liquid pressure, volume change upon solidification, and strain appearing in both solidifying and wall materials have been investigated, and the variation (elevation) in melting temperature has been theoretically determined in agreement with experiments on the system composed of Pb droplets in Al.[3] Likewise, phase field simulations have been performed for nonisothermal solidification and melting of confined spheres including internal stresses resulting from transformation in the confined volumes.[1] The temperature intervals where equilibrium states exist for the solid-liquid mixture have been then determined, their relative stability has been also investigated, and the surface energy has been estimated. In the framework of studies on diffusion-induced grain-boundary migration (DIGM) (Refs. 4–6 and references therein), the effect of coherency strain, resulting from solute diffusion ahead of the solidification front, has been investigated in a number of systems such as Mo-Ni or Al-Cu alloys, for example.[7,8] In the case of thin liquid film migration (LFM) where the coherency strain has been also identified as the driving force for the interface migration, a velocity selection theory of the growth of both solidification and melting fronts was developed by Brener and Temkin[9] including anisotropic surface-tension effects. Morphological evolution of solidification fronts due to solute concentration and/or thermal gradients has been also studied[10,11] as well as the stress-induced morphological instability for semi-infinite solids.[12,13] More recently, the coupling effect between these gradients and stress has been analyzed.[14,15] In this Brief Report, neglecting gravity effects, density changes, interfacial stress, and pressures in both phases, the growth of a spherical grain in contact with its melt in a pore embedded in a binary alloy solid matrix under stress has been investigated as well as the dissolution of the matrix. The condition on stress for the radial growth of the spheres has been first derived. A linear stability analysis has been then performed, and the morphological changes in both solidification and melting fronts have been analyzed.

A spherical grain of initial radius R_G^0 in contact with its melt is considered in a spherical pore of radius R_M^0, with $R_M^0 > R_G^0$, the effects of gravity being neglected (see Fig. 1 for the spherical coordinate system). Furthermore, the initial radius of the grain is assumed to be much larger than the critical nucleation radius whose determination is above the scope of the present study. Temperature is held fixed and diffusion of solute is assumed to occur in the liquid phase only whose concentration is labeled as C_L.[11] Changes in density upon solidification and melting are ignored as well as interfacial stress at both solidification and melting fronts. The reference state for stress is defined such that $|P_G| = |P_M| = |P_L| = 0$, where P_G, P_M, and P_L are the pressure terms in the grain, in the matrix, and in the liquid, respectively. The effect of liquid pressure is thus neglected. An additional constant stress $|T_0|$ ($|T_0| \gg |P_L|$) is then applied to the binary alloy matrix such that the nonzero components of the initial stress tensor $\tilde{T}^{(0)}$ are given by $T_{rr}^{(0)}(r,\theta,\varphi) = T_{\theta\theta}^{(0)}(r,\theta,\varphi) = T_{\varphi\varphi}^{(0)}(r,\theta,\varphi) = T_0$ when $r \to +\infty$. To determine the elastic relaxation in the neighborhood of the pore, the elastic displace-

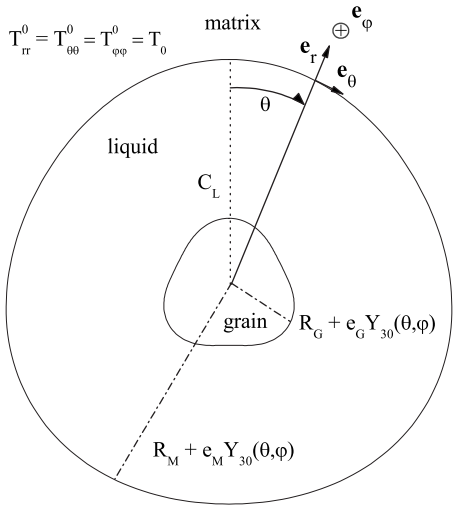

FIG. 1. A grain of initial radius R_G^0 in contact with its melt is considered in a pore of initial radius R_M^0 of a stressed matrix. Both solidification and dissolution fronts are perturbed with the help of the Y_{30} spherical harmonic. The amplitudes of the interface fluctuations for the grain and pore are labeled as e_G and e_M, respectively (the scale has been enlarged).

ment $\mathbf{u}^{(0)}$ in the solid matrix satisfying Navier's equation of equilibrium,[16]

$$\nabla^2\mathbf{u}^{(0)} + \frac{1}{1-2\nu}\nabla\cdot\nabla\mathbf{u}^{(0)} = 0, \tag{1}$$

has been taken to be of the form $\mathbf{u}^{(0)}(r,\theta,\varphi)=(\frac{A_0}{r^2}+B_0 r)\mathbf{e}_r$, with ν Poisson's ratio of the solid phase. The constants A_0 and B_0 have been determined using linear elasticity theory and writing the mechanical equilibrium equation as $\tilde{T}^{(0)}\cdot\mathbf{n_M}=0$ at the matrix interface $r=R_M^0$, where $\mathbf{n_M}$ is the outward normal pointing into the melt. The details of the straightforward calculation are not presented in this Brief Report and the components of the initial stress finally write[16]

$$T_{rr}^{(0)}(r,\theta,\varphi) = T_0\left(1-\frac{R_M^3}{r^3}\right), \tag{2}$$

$$T_{\theta\theta}^{(0)}(r,\theta,\varphi) = T_{\varphi\varphi}^{(0)}(r,\theta,\varphi) = T_0\left(1+\frac{R_M^3}{2r^3}\right). \tag{3}$$

The kinetics of the grain and matrix have been investigated in the hypothesis where the solute concentration C_L satisfies the Laplace equation,[11]

$$\nabla^2 C_L = 0. \tag{4}$$

The velocity of each solid-liquid interface is then defined as

$$v_{n_i}^i = \frac{D_L}{(C_S - C_L)|_{\text{int}}}\nabla C_L|_{\text{int}}\mathbf{n}_i, \tag{5}$$

with D_L as the diffusion coefficient in the liquid and $i=G,M$. In Eq. (5), the concentration of solute C_S and C_L in the solid and liquid phases, respectively, and the gradient of C_L are taken at the interfaces. The solute concentration is finally assumed to satisfy the Gibbs-Thomson equilibrium equations at the grain interface,[12,14,15,17,18]

$$\delta C_L = (C_L - C_L^0)|_{\text{int}} = \Gamma_L\kappa_G, \tag{6}$$

and at the matrix interface,

$$\delta C_L = (C_L - C_L^0)|_{\text{int}} = \Gamma_L\left[\kappa_M + \frac{\mathcal{G}}{\gamma}\right], \tag{7}$$

where κ_i is the curvature of the interface taken to be positive for the convex profile, with $i=G,M$, to be positive for the convex profile, and Γ_L is the constant defined by $\Gamma_L=\gamma T_M/(Lm)$, with T_M the melting temperature of the pure solvent, γ the constant interface energy per unit surface, L the latent heat per volume, and m as the liquidus slope assumed to be negative in the case where the solubility of solute in the solid is less than in the liquid, i.e., when the solute concentration in the liquid and solid phases at the corresponding stress-free planar interface, labeled as C_L^0 and C_S^0, respectively, satisfies $C_L^0 \geq C_S^0$. The elastic energy density $\mathcal{G}$ stored in the matrix is written as $\mathcal{G}=1/2T_{ij}E_{ij}$, with T_{ij} and E_{ij} the components of the stress and deformation tensors, respectively (summation over repeated indices is implied). In order to investigate the morphological evolution of both solid-liquid fronts during solidification and melting processes, a linear stability analysis has been performed as follows. Shape perturbation of the form $r_i(\theta,\varphi,t)=R_i+e_i(t)Y_{lm}(\theta,\varphi)$ has been introduced onto each interface, where e_i is the small fluctuation amplitude, with $i=G,M$, and $Y_{lm}(\theta,\varphi)$ is a spherical harmonic. The stress and solute concentrations have been then expressed to the first order in e_i as[18,19]

$$C_L(r,\theta,\varphi,t) = C_L^{(0)}(r) + C_L^{(1)}(r,\theta,\varphi,t) + \Theta(e_i^2), \tag{8}$$

$$T_{ij}(r,\theta,\varphi,t) = T_{ij}^{(0)}(r) + T_{ij}^{(1)}(r,\theta,\varphi,t) + \Theta(e_i^2), \tag{9}$$

with the following expression for the concentration fields that satisfy Eq. (4) (Refs. 18 and 20):

$$C_L^{(0)}(r) = \frac{C_0}{r} + D_0, \tag{10}$$

$$C_L^{(1)}(r,\theta,\varphi,t) = \left(C_1 r^l + \frac{D_1}{r^{l+1}}\right)e_i(t)Y_{lm}(\theta,\varphi). \tag{11}$$

In the framework of linear elasticity theory, the first-order correction in e_i of the stress $T_{ij}^{(1)}$ has been determined using the general expression of displacement field $\mathbf{u}^{(1)}$,[18,19]

$$u_r^{(1)}(r,\theta,\varphi,t) = f(r)e_i(t)Y_{lm}(\theta,\varphi), \tag{12}$$

$$u_\theta^{(1)}(r,\theta,\varphi,t) = g(r)e_i(t)\frac{\partial Y_{lm}}{\partial\theta}(\theta,\varphi), \tag{13}$$

$$u_\varphi^{(1)}(r,\theta,\varphi,t) = g(r)e_i(t)\frac{1}{\sin\theta}\frac{\partial Y_{lm}}{\partial\varphi}(\theta,\varphi), \tag{14}$$

with

$$f(r) = A_1 r^{-l-2} + B_1 r^{-l}, \tag{15}$$

$$g(r) = -\frac{1}{l+1}A_1 r^{-l-2} + \frac{4(1-\nu)-l}{l(l+3-4\nu)}B_1 r^{-l}. \tag{16}$$

The coefficients C_0, D_0, C_1, D_1, A_1, and B_1 have been determined expanding in power of e_i the mechanical equilibrium condition of both interfaces and Eqs. (6) and (7) and matching zero- and first-order terms, respectively. In the following, dimensionless radii $\tilde{R}_i=R_i/R_0$, perturbation amplitudes $\tilde{e}_i(t)=e_i(t)/e_i(0)$, and time $\tilde{t}=t/\tau$ have been used, where the distance R_0 and time constant τ are defined as

$$R_0 = \frac{8(1+\nu)}{9(1-\nu)}\frac{\mu\gamma}{T_0^2}, \quad \tau = \frac{R_0^3(C_S^0 - C_L^0)}{D_L\Gamma_L}, \tag{17}$$

with μ the shear modulus of the solid. Equation (5) has been then used to determine the time variation in the radii and perturbation amplitudes (to the first order in Γ_L) assuming that $\Gamma_L/(C_S-C_L)|_{\text{int}} \sim \Gamma_L/(C_S^0-C_L^0)$ which implies in particular that $|\Gamma_L|/R_i^0 \ll 1$ and $|\Gamma_L|/R_0 \ll 1$. In these restrictive hypotheses, one gets the following set of differential equations:

$$\frac{d\tilde{R}_G}{dt}(t) = \frac{\tilde{R}_M(t)\tilde{R}_G(t) - 2[\tilde{R}_G(t)+\tilde{R}_M(t)]}{\tilde{R}_G^2(t)[\tilde{R}_M(t)-\tilde{R}_G(t)]},$$

$$\frac{d\tilde{R}_M}{dt}(t) = \frac{\tilde{R}_M(t)\tilde{R}_G(t) - 2[\tilde{R}_G(t) + \tilde{R}_M(t)]}{\tilde{R}_M^2(t)[\tilde{R}_M(t) - \tilde{R}_G(t)]},$$

$$\frac{d\tilde{e}_G}{dt}(t) = \alpha_{11}\tilde{e}_G(t) + \alpha_{12}\tilde{e}_M(t),$$

$$\frac{d\tilde{e}_M}{dt}(t) = \alpha_{21}\tilde{e}_G(t) + \alpha_{22}\tilde{e}_M(t), \tag{18}$$

where the α_{ij}'s are four coefficients depending on $\tilde{R}_i$ radii whose expressions are not explicitly given in this Brief Report. From the first two equations of system (18), it can be deduced that both radii of grain and matrix satisfy $\tilde{R}_M^2(t)d\tilde{R}_M(t)/dt = \tilde{R}_G^2(t)d\tilde{R}_G(t)/dt$ leading to the relation $\tilde{R}_M^3(t) - \tilde{R}_G^3(t) = (\tilde{R}_M^0)^3 - (\tilde{R}_G^0)^3$ which states that for two growing concentric spheres, the difference of their radii to the third power is time independent. It can be emphasized that an analytic expression of the time dependence of the mean radius $\bar{R}$ can be determined in the case of growing isolated particles embedded in a matrix during Ostwald ripening or coarsening,[21–23] which is given by the well-known law of the form $\bar{R}^3(t) = \bar{R}^3(0) + \eta t$, with η a constant (independent of initial radii). Critical values of initial radii above which the grain grows and the matrix dissolves, i.e., when $d\tilde{R}_i(t)/dt > 0$, with $i = G, M$, can also be defined from the system of Eq. (18). It yields $\tilde{R}_M^0\tilde{R}_G^0 > 2(\tilde{R}_M^0 + \tilde{R}_G^0)$, with $\tilde{R}_M^0 > \tilde{R}_G^0$, which leads to the following conditions on dimensional initial radii:

$$R_M^0 > 4R_0, \tag{19}$$

$$R_G^0 > \frac{2R_0R_M^0}{(R_M^0 - 2R_0)}. \tag{20}$$

From Eqs. (19) and (20), a critical value T_0^c of stress can be also derived beyond which both spheres may grow,

$$T_0 > T_0^c = \frac{4}{3}\left(\frac{1+\nu}{1-\nu}\mu\gamma\right)^{1/2}\left(\frac{R_G^0 + R_M^0}{R_G^0R_M^0}\right)^{1/2}. \tag{21}$$

The opposite effects on interface velocity of stress and capillarity have been analyzed in Al(2.07 wt %)Cu alloy.[8] In particular, it has been shown that the composition stress in the grains being consumed during LFM or DIGM was to small to explain the observed curvatures developed in boundaries and liquid films. To study the effect of stress on the stability of both fronts, the above system of Eq. (18) has been solved numerically using standard techniques implemented in a calculus software.[24]

In the case of Al(2.07 wt %)Cu alloy where LFM has been experimentally observed and characterized during down-quench annealing for 60 s at $T = 863.15$ K,[8] one takes $E = 55.5$ GPa, $\nu = 0.345$ (at $T = 773.15$ K), $T_M = 933.47$ K, $L = 10.71 \times 10^8$ J m^{-3}, $\gamma = 0.163$ J m^{-2}, $C_S^0 \sim 1.4$ wt %, and $C_L^0 \sim 54$ wt %. For a given stress $T_0 \sim 50.0$ MPa, it yields $R_0 \sim 2.45 \times 10^{-6}$ m and $|\Gamma_L| = 6.72 \times 10^{-10}$ m. Taking then $\tilde{R}_M^0 = 10.0$ and $\tilde{R}_G^0 = 2.6$, one finds $|\Gamma_L|/R_0 \sim 2.74 \times 10^{-4}$, $|\Gamma_L|/R_M^0 \sim 2.74 \times 10^{-5}$, and $|\Gamma_L|/R_G^0 \sim 10^{-4}$ such that the conditions $|\Gamma_L|/R_i^0 \ll 1$ and $|\Gamma_L|/R_0 \ll 1$ used to derive the system of Eq. (18) are satisfied. In Fig. 2, both dimensionless radii $\tilde{R}_M$ and $\tilde{R}_G$ are found to increase as a function of time, according to Eqs. (19) and (20), leading thus to the radial growth of both spheres. In Fig. 3, the evolution of perturbation amplitudes has been then plotted versus time for the spherical harmonics corresponding to $l = 2, 3, 4$. It can be observed that the development of the first harmonic Y_{2m} breaking the spherical symmetry of the pore ($l = 1$ is a translational mode) appears to be limited on finite periods of time on both interfaces since its perturbation amplitude finally decreases with time onto the grain and matrix solid-liquid interfaces. However, for the higher-order spherical harmonics Y_{3m} and Y_{4m}, it can be observed that the corresponding amplitudes e_M increase with respect to time from $\tilde{t} = 0$, allowing stress-induced shape modification of the dissolution front. The fluctuations of amplitude e_G are also found to grow onto the solidification front but after a given relaxation time, the growing grain undergoing then a delayed morphological instability under the action of the applied stress generated in

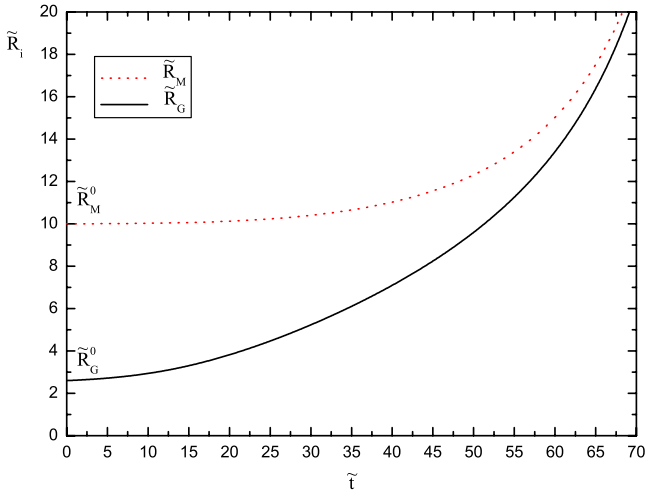

FIG. 2. (Color online) $\tilde{R}_i = R_i/R_0$ versus $\tilde{t} = t/\tau$, with $i = M, G$.

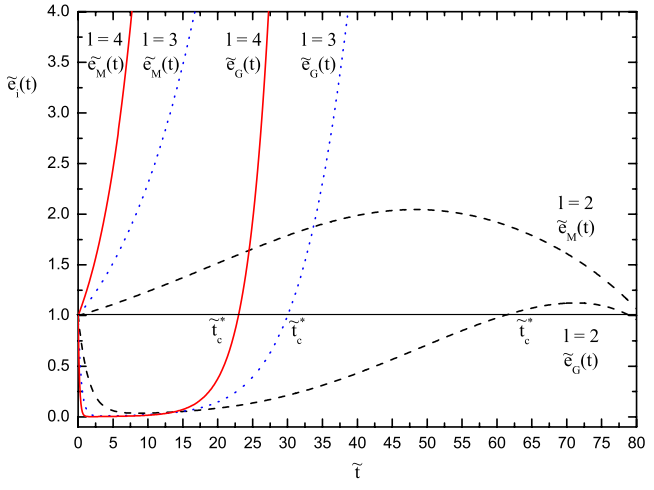

FIG. 3. (Color online) Dimensionless fluctuation amplitude $\tilde{e}_i$ versus $\tilde{t} = t/\tau$ for $l = 2, 3, 4$ and $i = M, G$.

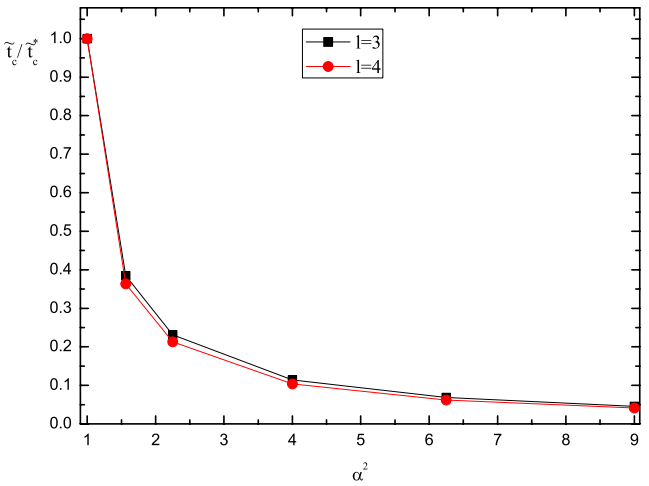

FIG. 4. (Color online) Variations in the delayed time ratio $\tilde{t}_c/\tilde{t}_c^*$ versus α^2 for $l=3$ and $l=4$.

the matrix. The effect of stress on the delayed time beyond which fluctuations develop on the grain interface has been finally investigated for $l=3$ and $l=4$ in Fig. 4. For each of these harmonics, the critical time ratio $\tilde{t}_c/\tilde{t}_c^*$ has been plotted as a function of $\tilde{R}_i^0/\tilde{R}_i^{0,*}=\alpha^2$, with $i=G,M$, where the dimensionless critical time $\tilde{t}_c^*$ and radii $\tilde{R}_i^{0,*}$ correspond to the case already studied, i.e., for $\tilde{R}_M^{0,*}=10.0$ and $\tilde{R}_G^{0,*}=2.6$ at a given stress T_0^*, with α the coefficient being defined from initial stresses as $T_0=\alpha T_0^*$. From this scaling, only one curve can be considered from the numerical point of view for both harmonics $l=3,4$ as displayed in Fig. 4. The destabilizing effect of stress can be then again emphasized since it is found that for these two spherical harmonics, the critical time beyond which the delayed morphological change in the grain interface takes place rapidly decreases with stress.

In conclusion, it has been demonstrated that an applied stress to the matrix may counterbalance the capillarity effects and may then be the driving force for the radial growth of the grain and the dissolution of the matrix. A linear stability analysis has then shown that the stress may be responsible for the development of roughness onto the matrix dissolution front. A delayed roughness has been also found to develop onto the grain solidification front due to the stress generated in the matrix. Finally, it can be emphasized that it would be a challenge to investigate the effects of stress onto the morphological changes in both fronts in their nonlinear regime of evolution using numerical approaches such as phase field methods, for example.

*Permanent address: PHYMAT, UMR 6630 CNRS, Université de Poitiers, BP 30179, 86962 Futuroscope Cedex, France. jerome.colin@univ-poitiers.fr

[1] J. Slutsker, K. Thornton, A. L. Roytburd, J. A. Warren, and G. B. McFadden, Phys. Rev. B **74**, 014103 (2006).
[2] E. Cho, J. J. Ko, H. Y. Ha, S. A. Hong, K. Y. Lee, T. W. Lim, and I. H. Oh, J. Electrochem. Soc. **150**, A1667 (2003).
[3] J. J. Hoyt, Phys. Rev. Lett. **96**, 045702 (2006).
[4] M. Hillert, Scr. Metall. **17**, 237 (1983).
[5] D. N. Yoon, J. W. Cahn, C. A. Handwerker, J. E. Blendell, and Y. J. Baik, *Interface Migration and Control of Microstructures* (American Society for Metals, Metals Park, OH, 1985), pp. 19–31.
[6] D. N. Yoon, Int. Mater. Rev. **40**, 149 (1995).
[7] D. N. Yoon and W. J. Hupmann, Acta Metall. **27**, 973 (1979).
[8] M. Kuo and R. A. Fournelle, Acta Metall. Mater. **39**, 2835 (1991).
[9] E. A. Brener and D. E. Temkin, Phys. Rev. Lett. **94**, 184501 (2005).
[10] W. W. Mullins and R. F. Sekerka, J. Appl. Phys. **35**, 444 (1964).
[11] W. W. Mullins and R. F. Sekerka, J. Appl. Phys. **34**, 323 (1963).
[12] R. J. Asaro and W. A. Tiller, Metall. Trans. **3**, 1789 (1972).
[13] M. A. Grinfeld, Dokl. Akad. Nauk SSSR **290**, 1358 (1986).
[14] I. Durand, K. Kassner, C. Misbah, and H. Müller-Krumbhaar, Phys. Rev. Lett. **76**, 3013 (1996).
[15] I. Cantat, K. Kassner, C. Misbah, and H. Müller-Krumbhaar, Phys. Rev. E **58**, 6027 (1998).
[16] I. S. Sokolnikoff, *Mathematical Theory of Elasticity*, 2nd ed. (McGraw-Hill, New York, 1956).
[17] F. Larché and J. W. Cahn, Acta Metall. **21**, 1051 (1973).
[18] B. Caroli, C. Caroli, B. Roulet, and P. W. Voorhees, Acta Metall. **37**, 257 (1989).
[19] P. H. Leo, J. Iwan, D. Alexander, and R. K. Serkerka, Acta Metall. **33**, 985 (1985).
[20] B. A. Boley and J. H. Weiner, *Theory of Thermal Stresses* (Wiley, New York, 1960).
[21] I. M. Lifshitz and V. V. Slyozov, J. Phys. Chem. Solids **19**, 35 (1961).
[22] C. Wagner, Z. Elektrochem. **65**, 581 (1961).
[23] K. Thornton, N. Akaiwa, and P. W. Voorhees, Phys. Rev. Lett. **86**, 1259 (2001).
[24] MATHEMATICA, Version 5.1, Wolfram Research, Inc., Champaign, IL, 2004.